X-ray emission from isolated neutron stars: latest results from XMM-Newton and NICER data

MICHELA RIGOSELLI[1]

Sandro Mereghetti[1], Davide De Grandis[1], Roberto Turolla[2,3], Roberto Taverna[2], Silvia Zane[3], George Younes[4], Andrea Tiengo[1,5], Sara Anzuinelli[1,6], Luca Baldeschi[1,7]

29/09/2022 — Cefalù

1 INAF, Istituto di Astrofisica Spaziale e Fisica Cosmica Milano
2 Dipartimento di Fisica e Astronomia, Università di Padova
3 MSSL-UCL
4 Department of Physics, The George Washington University
5 Scuola Universitaria Superiore IUSS Pavia
6 Dipartimento di Fisica, Università degli Studi di Milano-Bicocca
7 Dipartimento di Fisica, Università degli Studi di Milano

Bolometric thermal luminosity vs age

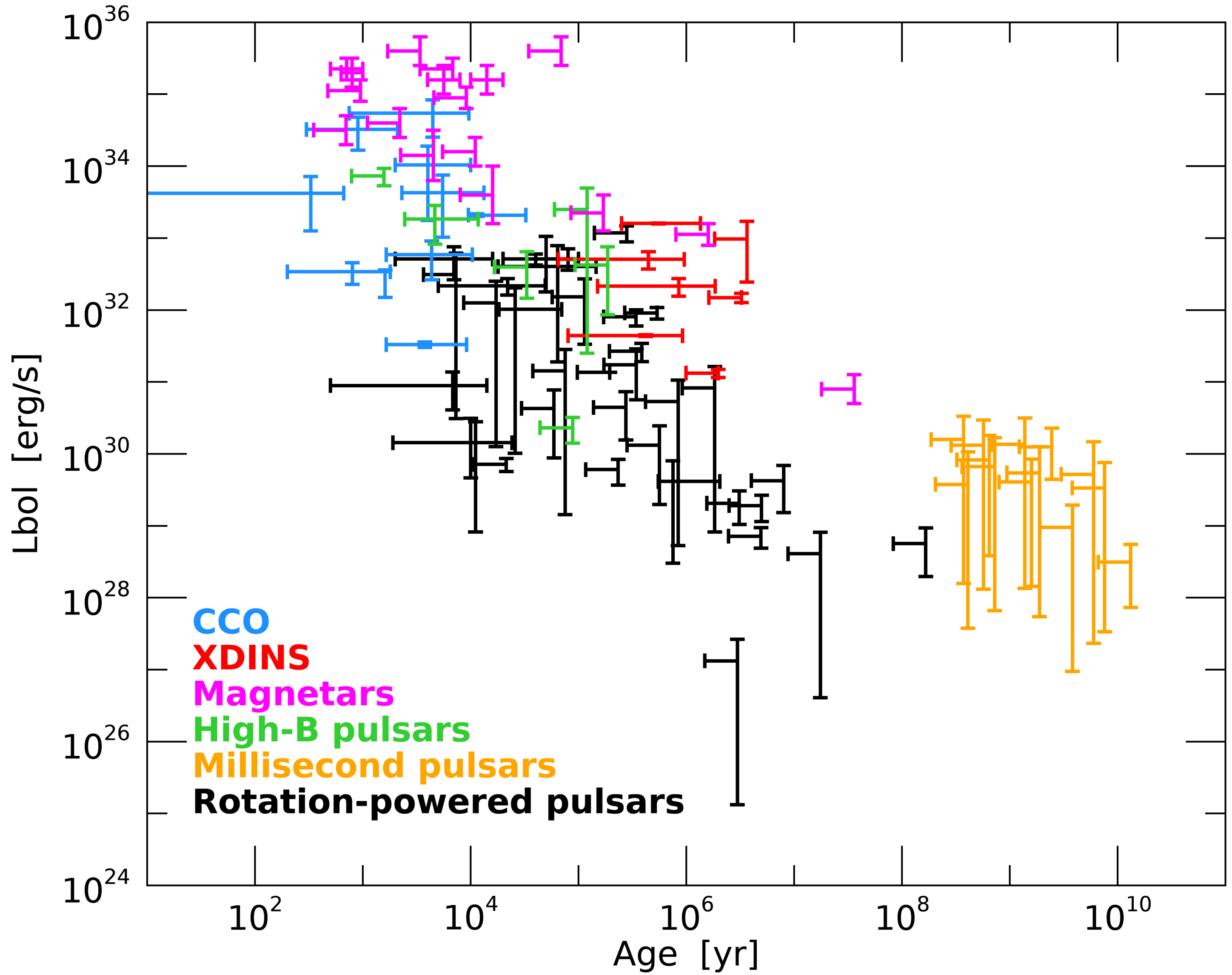

see also Potekhin+ 2020, MNRAS

Bolometric thermal luminosity vs age

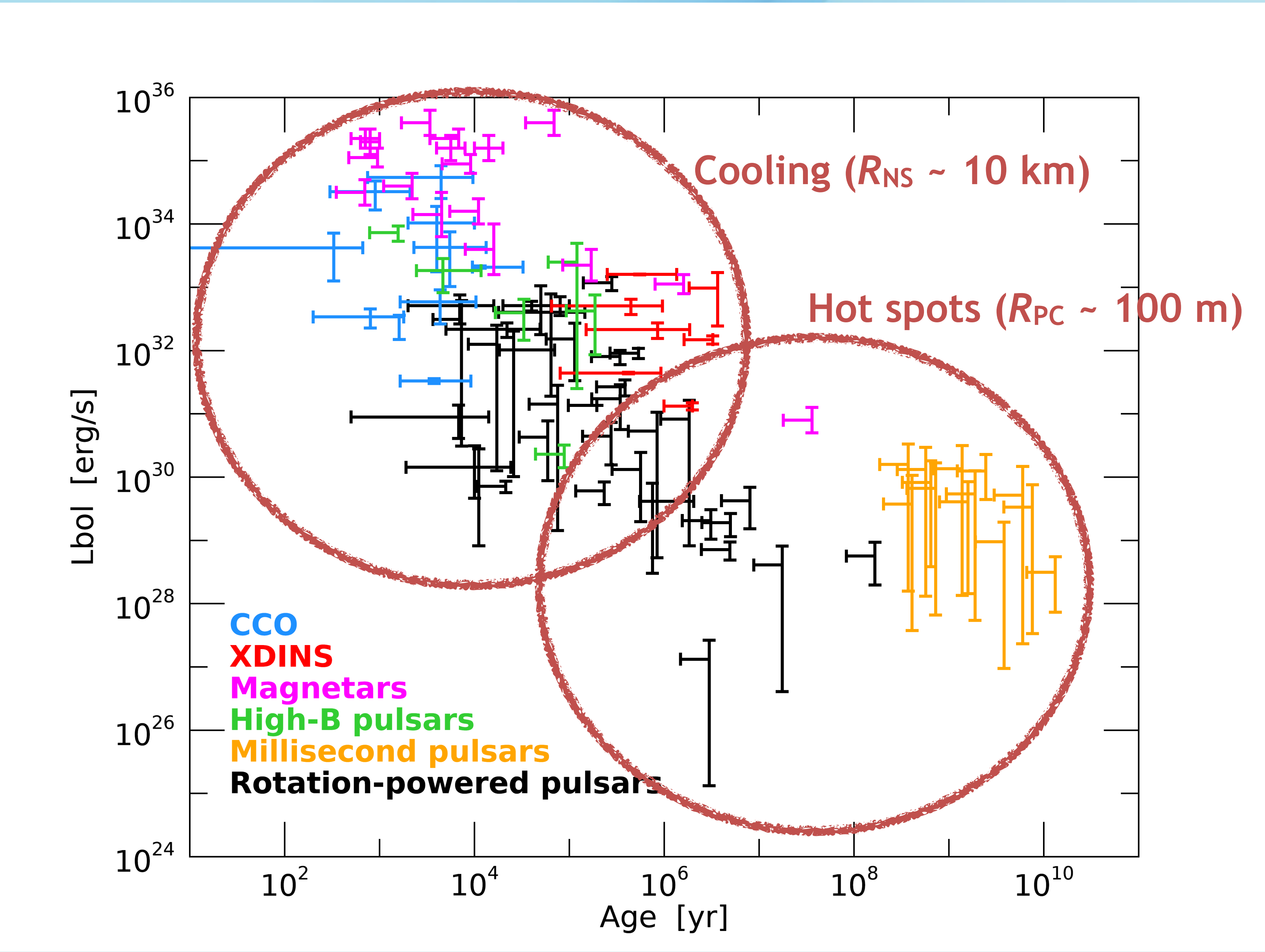

see also Potekhin+ 2020, MNRAS

Thermal emission models: theory…

- Multi-temperature surface, function of *B* field
- Local emissivity function of composition (gas and/or ions) and of *B* field
- Integrated emissivity depends on GR effects (function of M/R) and on emission geometry (X and ξ, emitting area…)

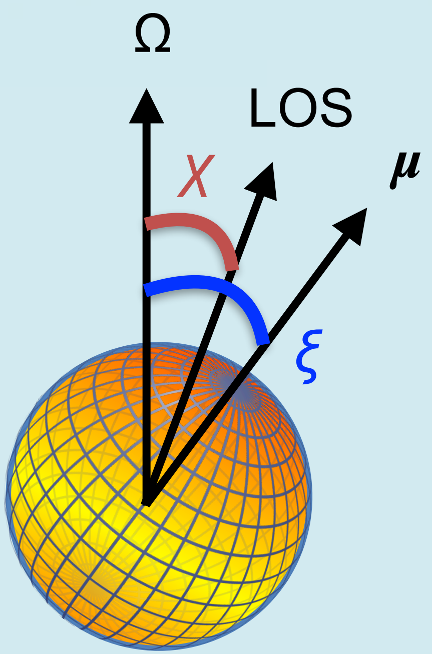

Lloyd+ 2003, ApJ
Potekhin+ 2004, 2012, 2014 A&A
Suleimanov+ 2009, 2010 A&A
Taverna+ 2015, MNRAS
Zane & Turolla 2006, MNRAS

Thermal emission models: …vs practice!

~60 thermal INSs:

- ~40 fitted with 1BB
- ~20 fitted with 2BB

(one to account for the cooler and larger part of the surface, the other to account for the hotter region or the heated hot spot)

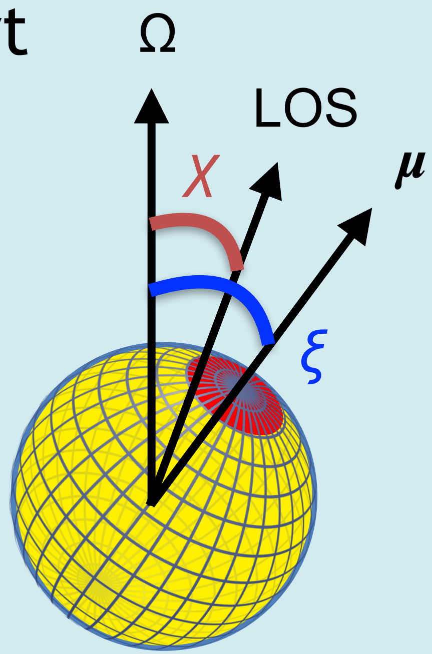

Rigoselli+ 2022b, MNRAS

2BB thermal INSs

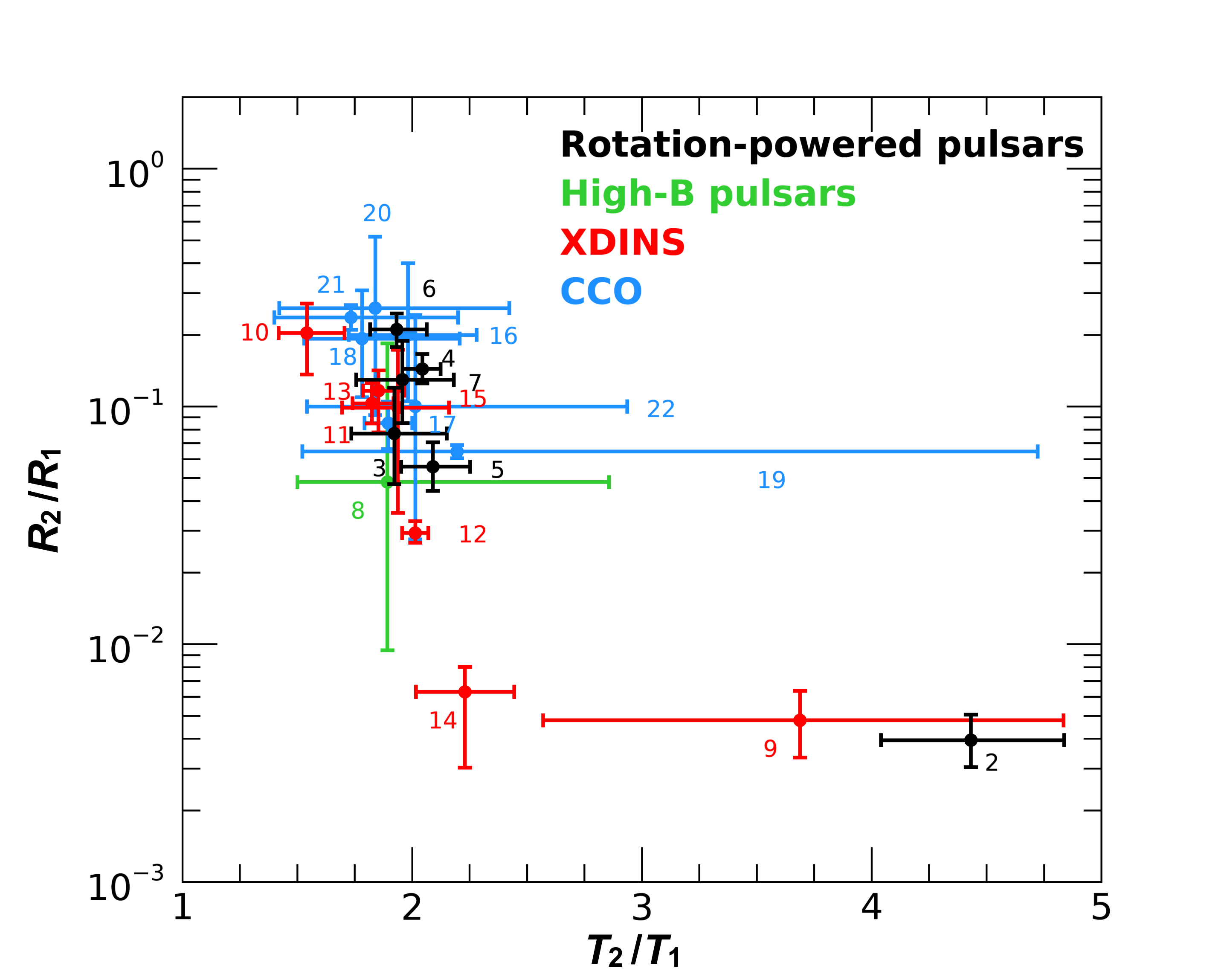

RPP: #1 PSR J0633+1746, #2 PSR B0656+14, #3 PSR B0833-45, #4 PSR B1055-52, #5 1RXS J141256.0+792204, #6 PSR J1740+1000;
High-B PSR: #7 PSR J0726-2612; XDINS: #8 RX J0420.0−5022, #9 RX J0720.4−3125, #10 RX J0806.4−4123, #11 RX J1308.6+2127, #12 RX J1605.3+3249, #13 RX J1856.5-3754, #14 RX J2143.0+0654; CCO: #15 RX J0822.0−4300, #16 1E 1207.4−5209, #17 1WGA J1713.4−3949, #18 XMMU J172054.5−372652, #19 XMMU J173203.3−344518, #20 CXOU J185238.6+004020, #21 CXOU J232327.9+584842

Rigoselli+ 2022b, MNRAS

2BB thermal INSs

$T_2/T_1 \sim 2$
$R_2/R_1 \sim 0.02 - 0.5$

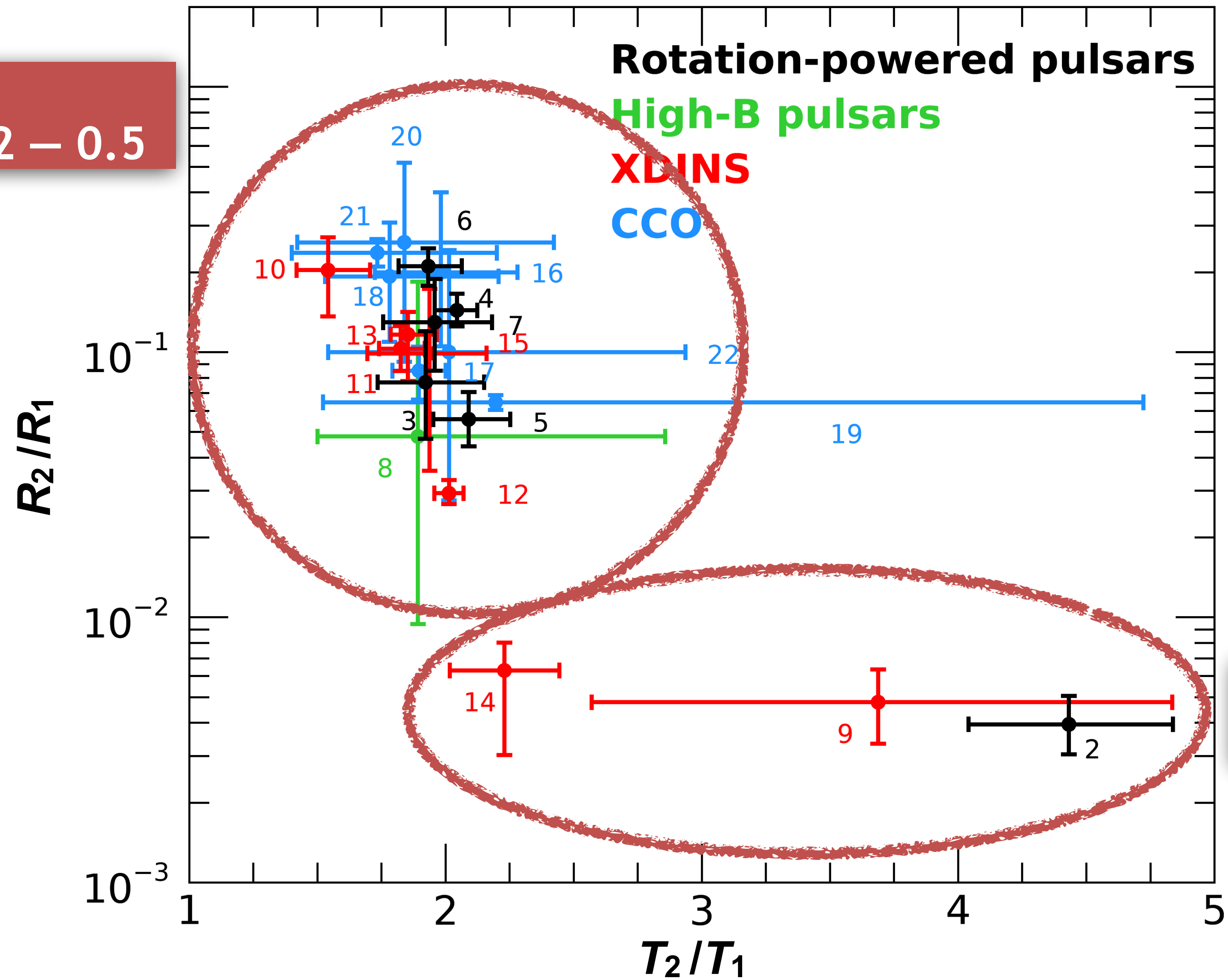

$T_2/T_1 \sim 2 - 5$
$R_2/R_1 \sim 0.005$

RPP: #1 PSR J0633+1746, #2 PSR B0656+14, #3 PSR B0833-45, #4 PSR B1055-52, #5 1RXS J141256.0+792204, #6 PSR J1740+1000;
High-B PSR: #7 PSR J0726-2612; XDINS: #8 RX J0420.0−5022, #9 RX J0720.4−3125, #10 RX J0806.4−4123, #11 RX J1308.6+2127, #12 RX J1605.3+3249, #13 RX J1856.5-3754, #14 RX J2143.0+0654; CCO: #15 RX J0822.0−4300, #16 1E 1207.4−5209, #17 1WGA J1713.4−3949, #18 XMMU J172054.5−372652, #19 XMMU J173203.3−344518, #20 CXOU J185238.6+004020, #21 CXOU J232327.9+584842

The XDINSs, purely thermal NSs

P, $\dot{P}$ —> τ_c ~ 10^6 yr, B_s ~ 10^{13} G, $\dot{E}_{ROT}$ ~ 10^{30} - 10^{31} erg/s

Source name	L_X	$10^{-3}\ \dot{E}_{ROT} / 4\pi d^2$	Spectrum
RX	10^{32} erg/s	10^{-15} erg/cm^2/s	Yoneyama+ 2019
J0420.0–5022	0.13±0.02	1.8	2BB
J0720.4–3125	2.1±0.6	0.5	G*2BB
J0806.4–4123	1.5±0.2	0.2	G*2BB
J1308.6+2127	16.0±0.2	0.13	G*2BB
J1605.3+3249	5.1±1.4	—	G*2BB
J1856.5–3754	0.44±0.01	1.8	2BB
J2143.0+0654	9.7±7.3	0.09	G*2BB

The XDINSs, purely ~~thermal~~ NSs

P, $\dot{P}$ —> τ_c ~ 10^6 yr, B_s ~ 10^{13} G, $\dot{E}_{ROT}$ ~ 10^{30} - 10^{31} erg/s

Source name	L_X	$10^{-3}\ \dot{E}_{ROT} / 4\pi d^2$	Spectrum
RX	10^{32} erg/s	10^{-15} erg/cm^2/s	~~Yoneyama+ 2019~~ De Grandis, MR+ 2022b
J0420.0–5022	0.13±0.02	1.8	2BB+PL
J0720.4–3125	2.1±0.6	0.5	G*2BB
J0806.4–4123	1.5±0.2	0.2	G*2BB
J1308.6+2127	16.0±0.2	0.13	G*2BB
J1605.3+3249	5.1±1.4	—	G*2BB
J1856.5–3754	0.44±0.01	1.8	2BB+PL
J2143.0+0654	9.7±7.3	0.09	G*2BB

see also Dessert+ 2020, ApJ

RX J0420.0—5022: Spectral analysis

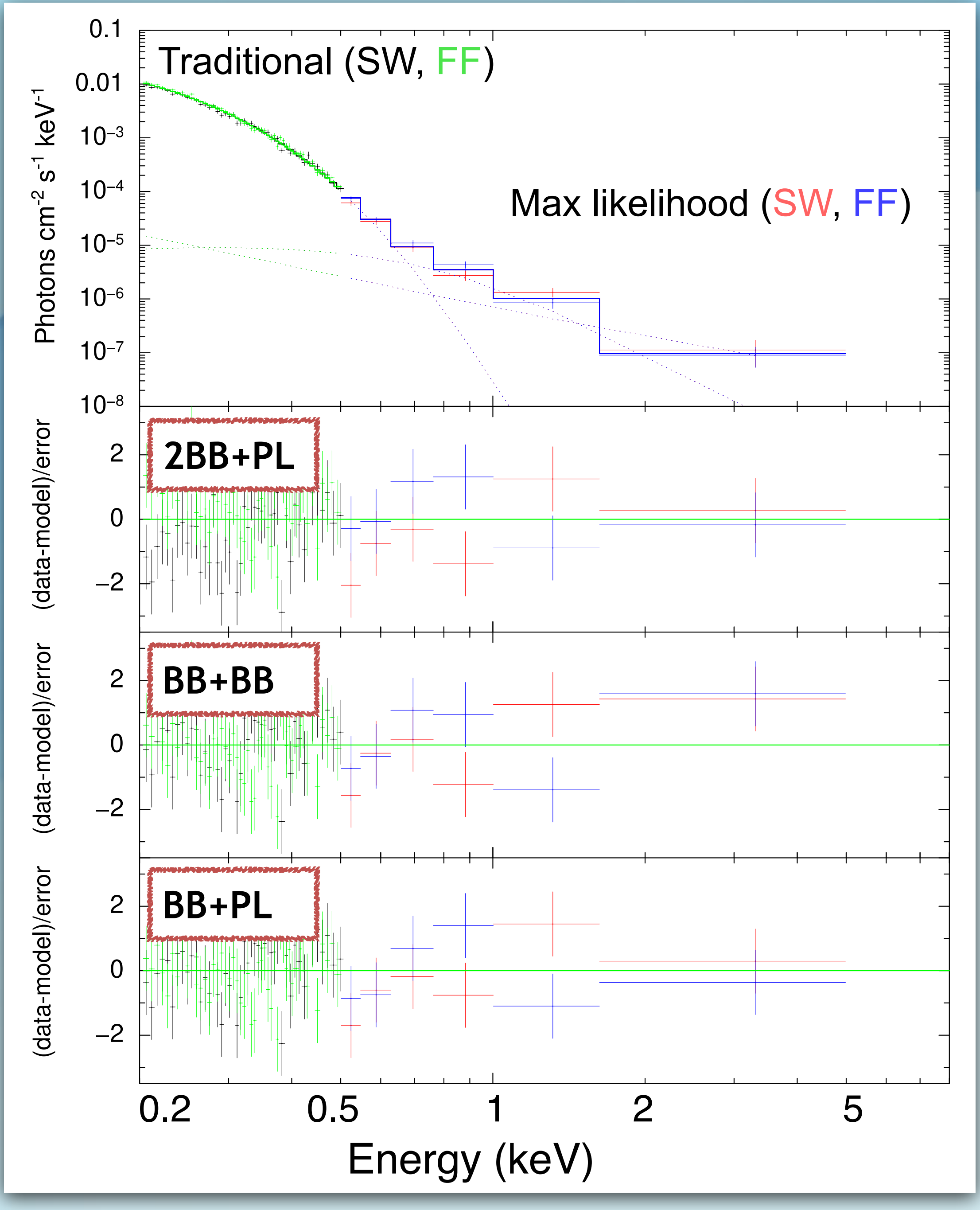

- 20 years of *XMM-Newton* data [144 ksec]
- Bulk of emission: BB with kT_1=46.3±0.3 eV, R_1=4.6±0.2 km
- Hard excess extracted with a maximum likelihood method…
- … and fitted with a second BB (kT_2~210 eV, R_2~17 m), or a PL (Γ~3.1, F~10^{-15} erg/cm^2/s), or both (kT_2~170 eV, Γ~1.6)

De Grandis, MR+ 2022b, MNRAS

RX J1856.5—3754: Spectral analysis

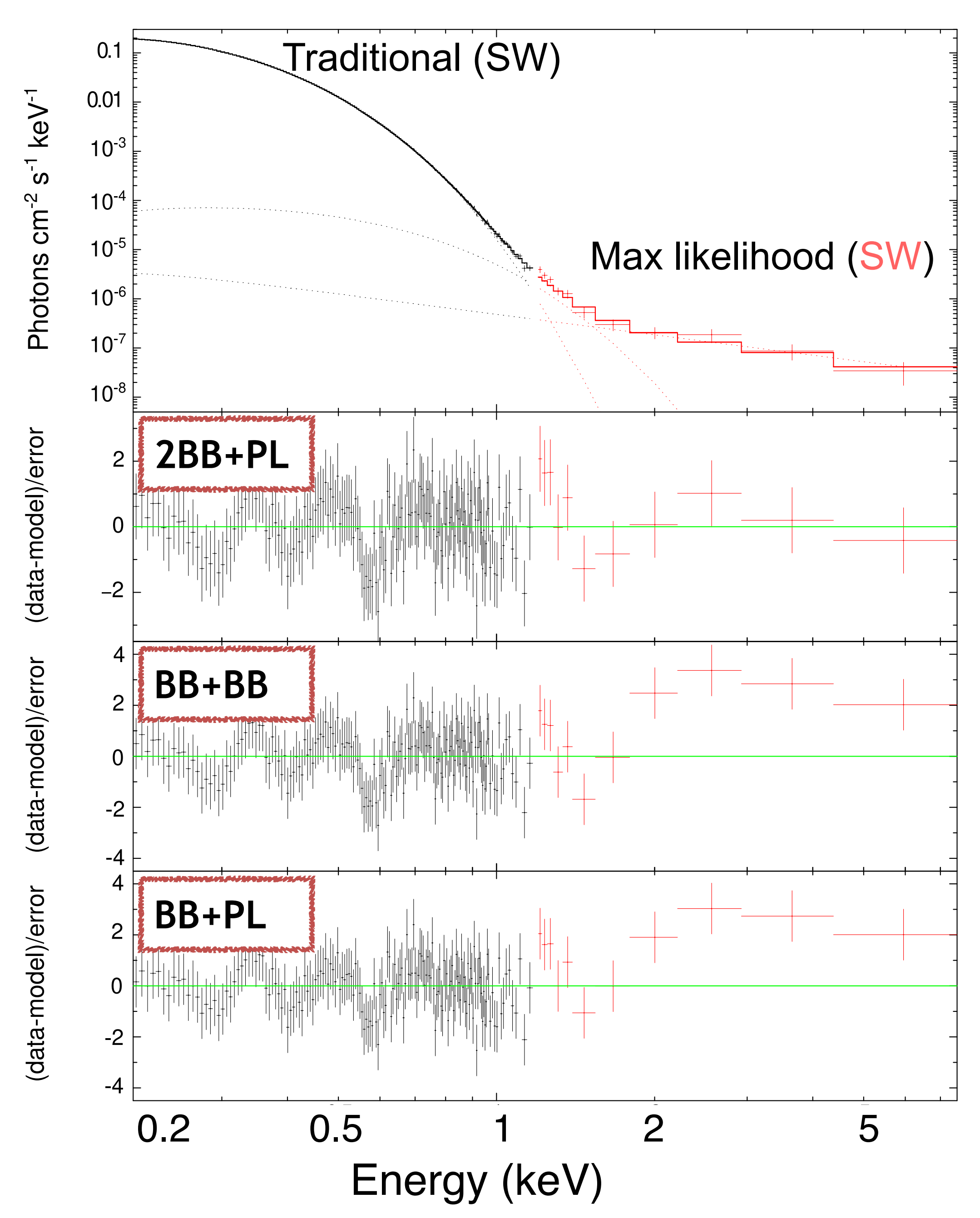

- 20 years of *XMM-Newton* data [1.43 Msec]
- Bulk of emission: BB with kT_1=61.9±0.1 eV, R_1=4.92±0.05 km
- Hard excess extracted with a maximum likelihood method…
- … and fitted with a second BB (kT_2=138±13 eV, R_2=31±12 m) plus a PL (Γ~1.4±0.5, F~(2.5±0.7)x10^{-15} erg/cm^2/s)

De Grandis, MR+ 2022b, MNRAS

RX J1856.5—3754: Timing solution

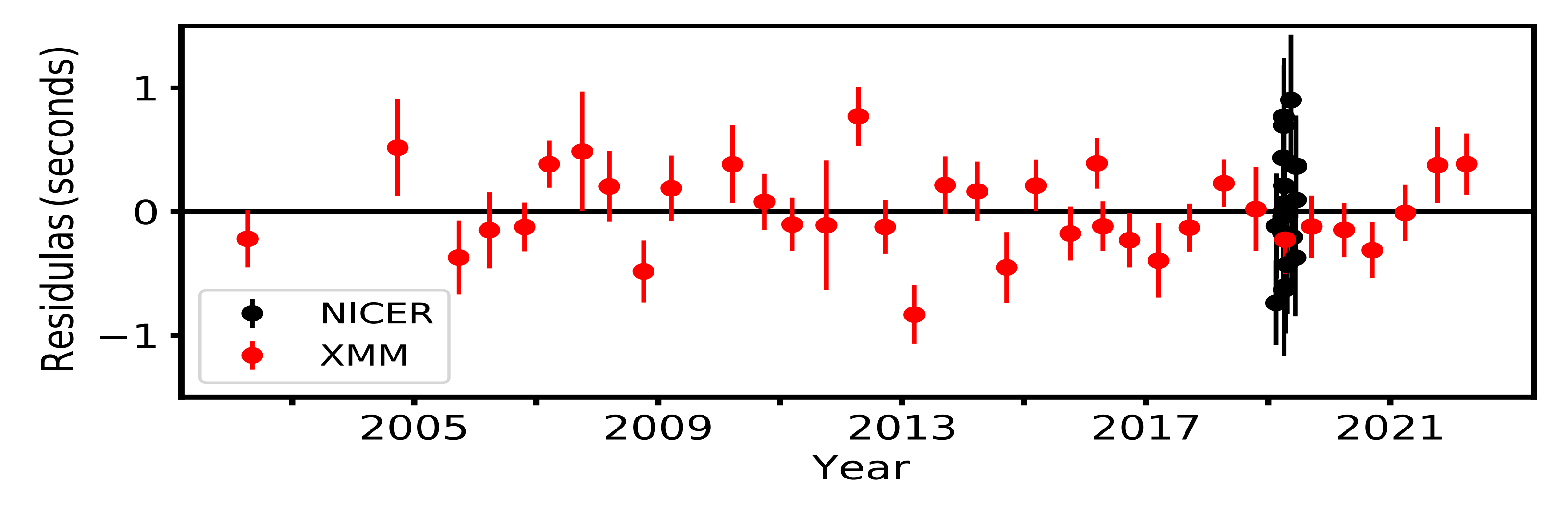

- Coherent timing solution with no more cycles ambiguity
- A stable solution throughout 20 years (ν = 0.14173907778(8) Hz, $\dot{\nu}$ = −6.042(4)×10^{-16} Hz/s, $|\ddot{\nu}|$< 10^{-26} Hz/s^2)
- Non symmetric pulse profile

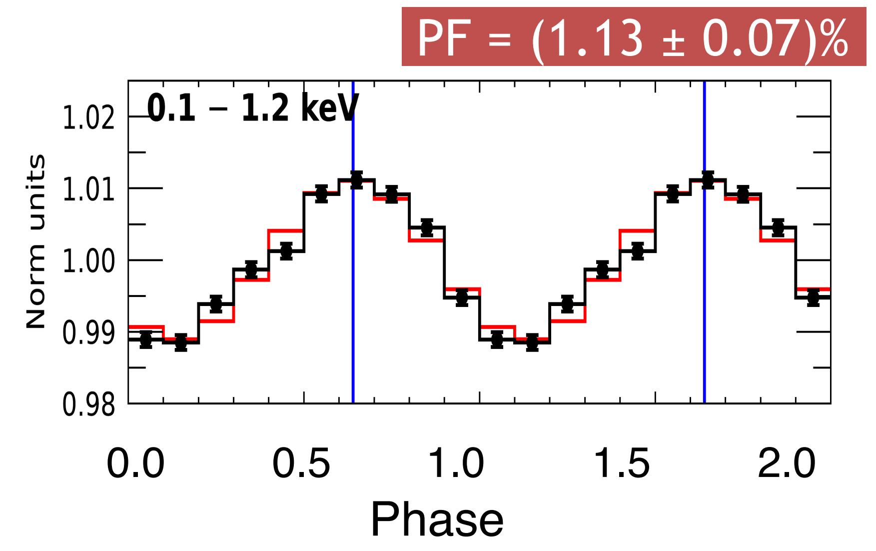

De Grandis, MR+ 2022b, MNRAS

RX J1856.5—3754: Pulse profiles

Soft pulse profile

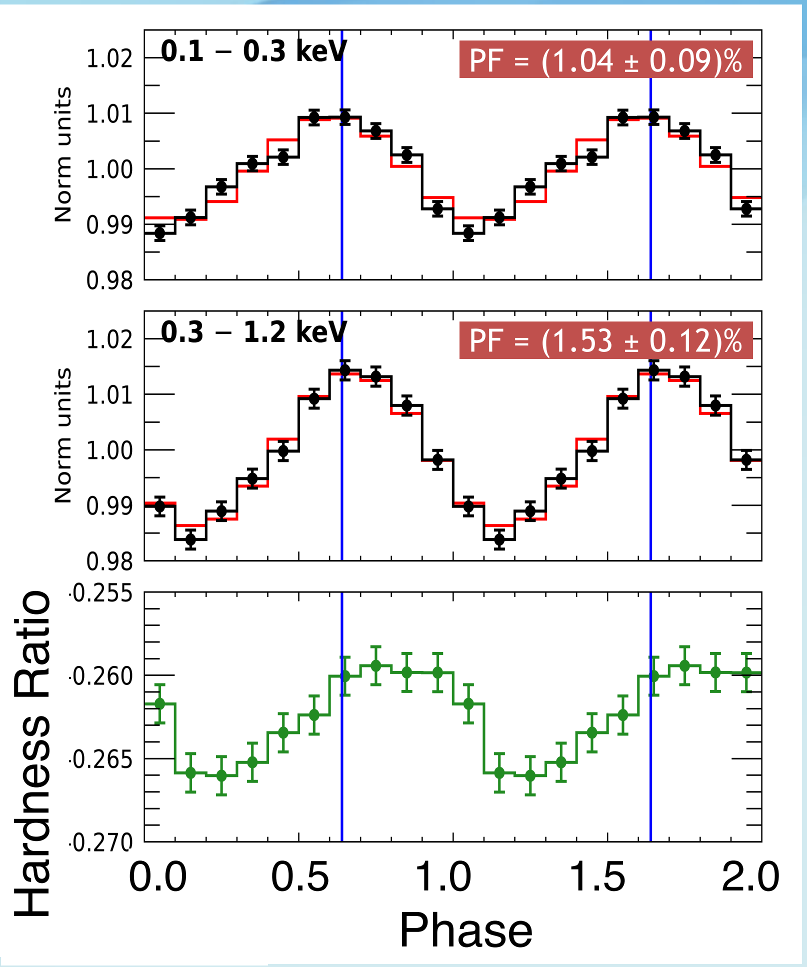

Hard pulse profile

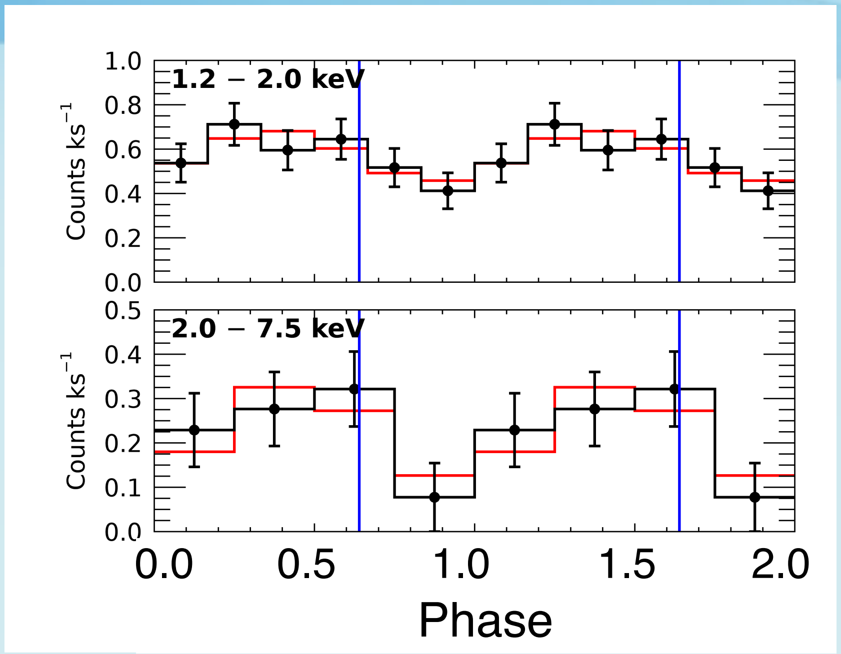

- Statistically significant variation in the hardness ratio: the spectrum gets harder at the peak of the pulse profile
- Hints of pulsation also above 1 keV

De Grandis, MR+ 2022b, MNRAS

Thermal emission models: simulations!

- We simulated with a *MCMC* approach thermal spectra assuming a certain T distribution and T_{p}, a local emissivity, a compactness, an emission geometry
- We fitted those spectra with 2BB model, we measured the resulting T_2/T_1 and R_2/R_1, and we compared the results with the data

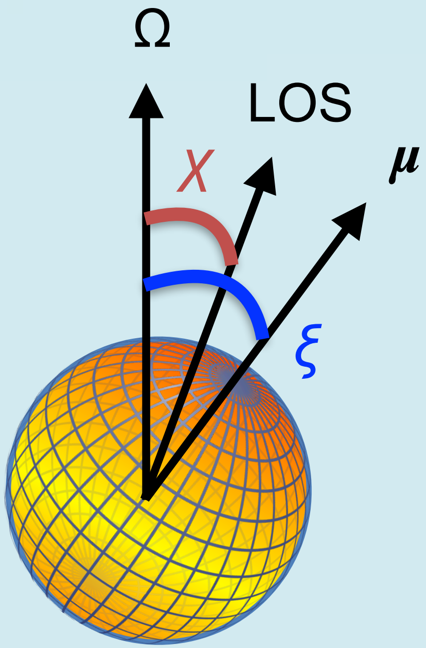

2BB thermal INSs

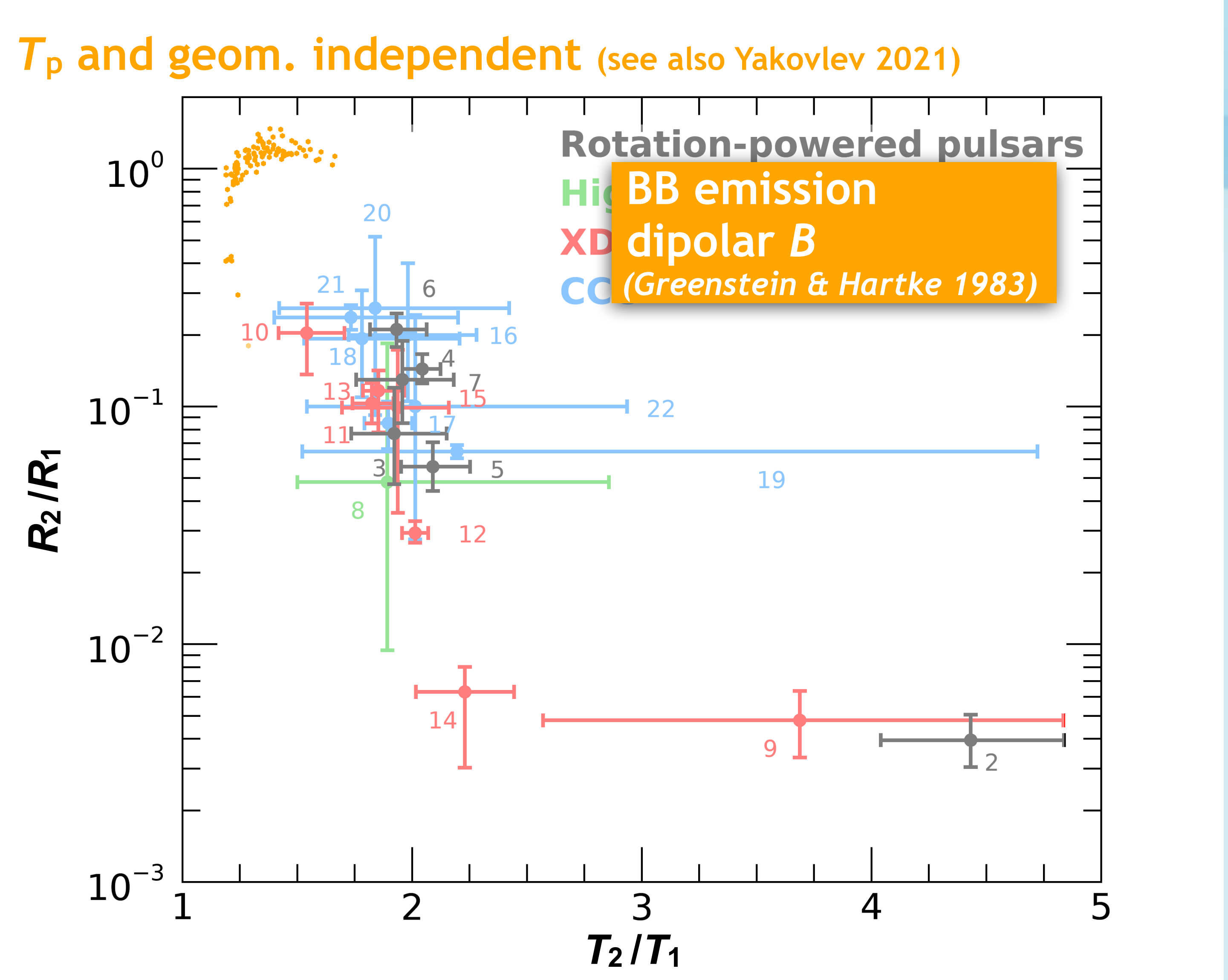

RPP: #1 PSR J0633+1746, #2 PSR B0656+14, #3 PSR B0833-45, #4 PSR B1055-52, #5 1RXS J141256.0+792204, #6 PSR J1740+1000;
High-B PSR: #7 PSR J0726-2612; XDINS: #8 RX J0420.0−5022, #9 RX J0720.4−3125, #10 RX J0806.4−4123, #11 RX J1308.6+2127, #12 RX J1605.3+3249, #13 RX J1856.5-3754, #14 RX J2143.0+0654; CCO: #15 RX J0822.0−4300, #16 1E 1207.4−5209, #17 1WGA J1713.4−3949, #18 XMMU J172054.5−372652, #19 XMMU J173203.3−344518, #20 CXOU J185238.6+004020, #21 CXOU J232327.9+584842

Rigoselli+ 2022b, MNRAS

2BB thermal INSs

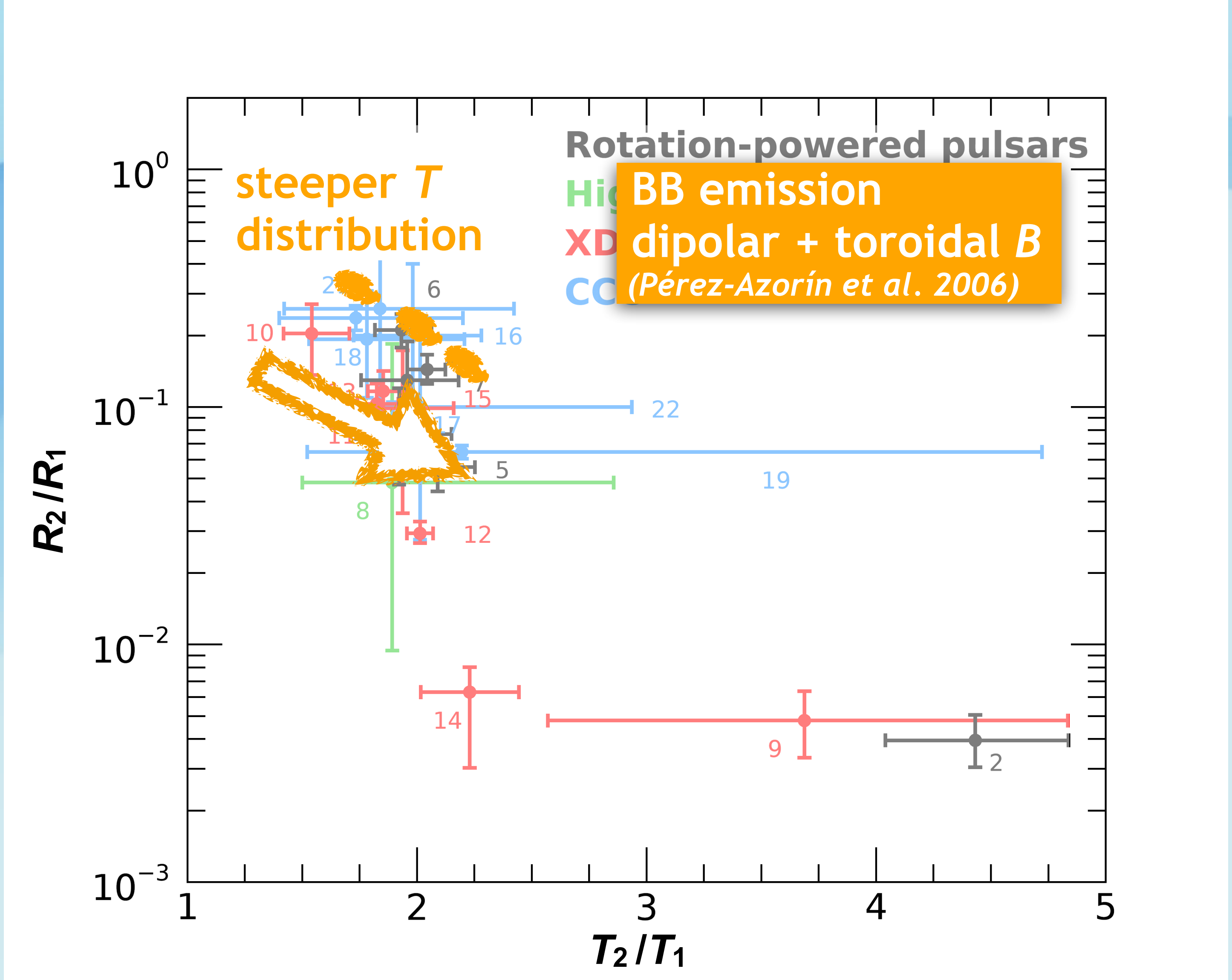

RPP: #1 PSR J0633+1746, #2 PSR B0656+14, #3 PSR B0833-45, #4 PSR B1055-52, #5 1RXS J141256.0+792204, #6 PSR J1740+1000; High-B PSR: #7 PSR J0726-2612; XDINS: #8 RX J0420.0−5022, #9 RX J0720.4−3125, #10 RX J0806.4−4123, #11 RX J1308.6+2127, #12 RX J1605.3+3249, #13 RX J1856.5-3754, #14 RX J2143.0+0654; CCO: #15 RX J0822.0−4300, #16 1E 1207.4−5209, #17 1WGA J1713.4−3949, #18 XMMU J172054.5−372652, #19 XMMU J173203.3−344518, #20 CXOU J185238.6+004020, #21 CXOU J232327.9+584842

Rigoselli+ 2022b, MNRAS

2BB thermal INSs

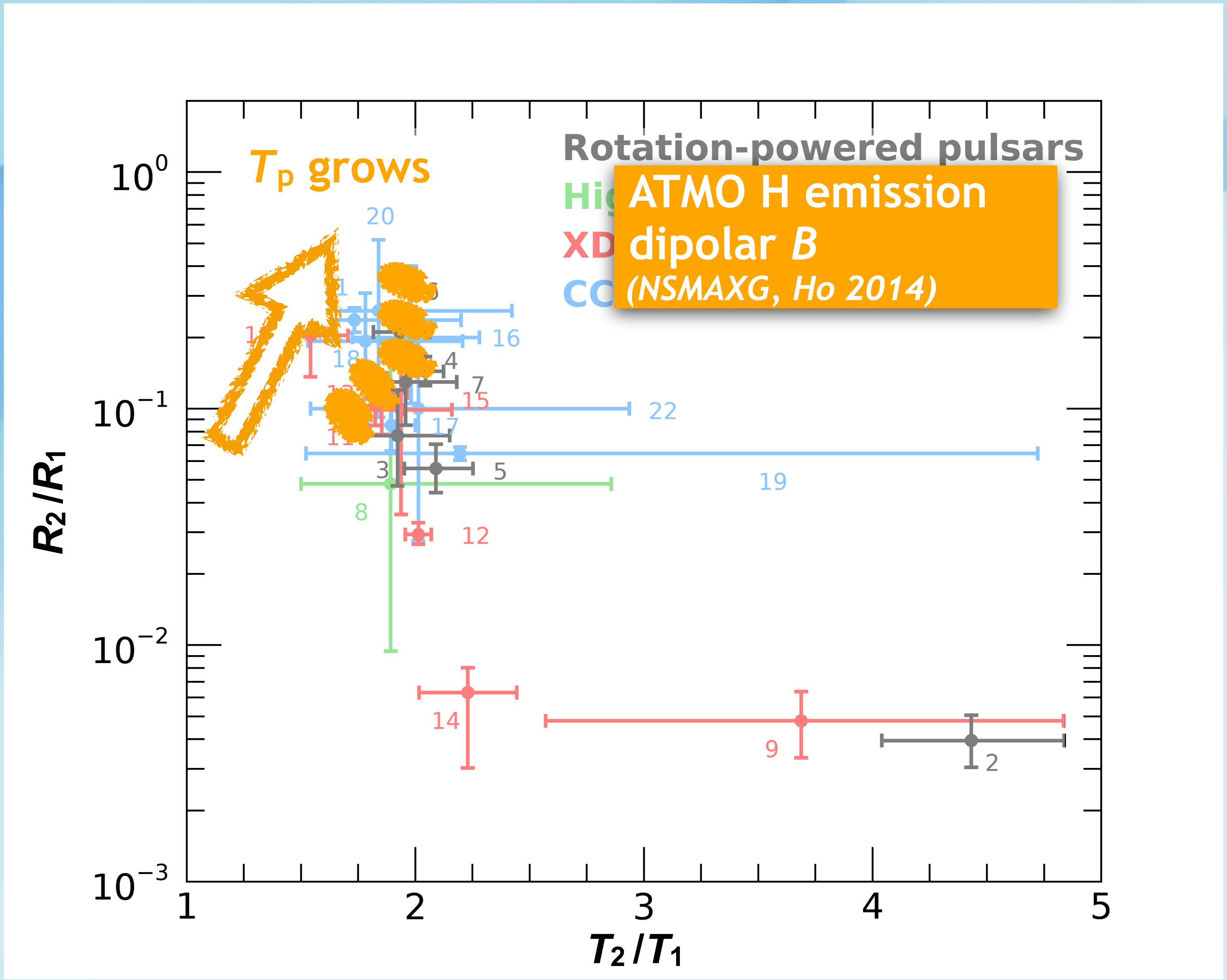

RPP: #1 PSR J0633+1746, #2 PSR B0656+14, #3 PSR B0833-45, #4 PSR B1055-52, #5 1RXS J141256.0+792204, #6 PSR J1740+1000;
High-B PSR: #7 PSR J0726-2612; XDINS: #8 RX J0420.0−5022, #9 RX J0720.4−3125, #10 RX J0806.4−4123, #11 RX J1308.6+2127, #12 RX J1605.3+3249, #13 RX J1856.5-3754, #14 RX J2143.0+0654; CCO: #15 RX J0822.0−4300, #16 1E 1207.4−5209, #17 1WGA J1713.4−3949, #18 XMMU J172054.5−372652, #19 XMMU J173203.3−344518, #20 CXOU J185238.6+004020, #21 CXOU J232327.9+584842

Conclusions

- The XDINS class is probably more variegate than previously thought. We just reached the minimum sensitivity needed to detect their non-thermal component, if present.

- The "T_2/T_1 vs R_2/R_1" plot is a roadmap to interpret the thermal emission of INSs, which seem to share a common T distribution despite a different evolutionary stage. Geminga, J0420 and J1856 are the exceptions: they have small hot spots heated by magnetospheric currents.

- The plot can also be used to test theoretical models. Magnetized atmosphere models with steep T distributions are needed.

Thanks for the attention!

T distribution

$$T^4(\theta) = T_{\rm p}^4 \frac{\cos^2\theta}{\cos^2\theta + \alpha\sin^2\theta} + T_{\rm min}^4$$

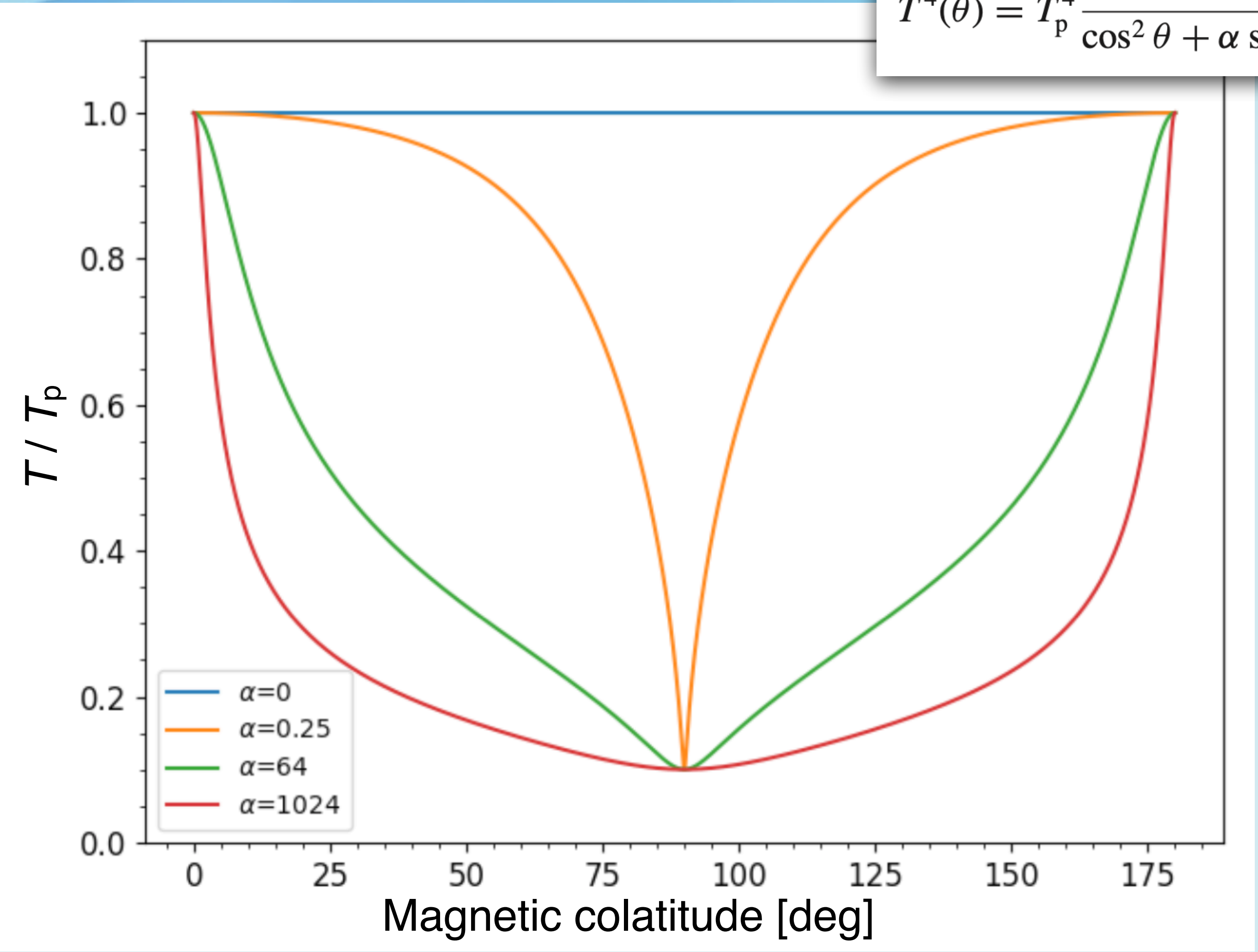

The XDINSs, purely ~~thermal~~ NSs

P, $\dot{P}$ —> τ_c ~ 10^6 yr, B_s ~ 10^{13} G, $\dot{E}_{ROT}$ ~ 10^{30} - 10^{31} erg/s

Source name	L_X	$10^{-3}\ \dot{E}_{ROT}\ /\ 4\pi d^2$	E_{cyc}	Spectrum
RX	10^{32} erg/s	10^{-15} erg/cm²/s	eV	Yoneyama+ 2019 De Grandis, MR+ 2022b
J0420.0–5022	0.13±0.02	1.8	—	2BB+PL
J0720.4–3125	2.1±0.6	0.5	255±30	G*2BB
J0806.4–4123	1.5±0.2	0.2	240±10	G*2BB
J1308.6+2127	16.0±0.2	0.13	390±6	G*2BB
J1605.3+3249	5.1±1.4	—	350±50	G*2BB
J1856.5–3754	0.44±0.01	1.8	—	2BB+PL
J2143.0+0654	9.7±7.3	0.09	325±70	G*2BB

see also Dessert+ 2020, ApJ

Effective area